Heliyon 10 (2024) e31856

Contents lists available at ScienceDirect

Heliyon

journal homepage: www.cell.com/heliyon

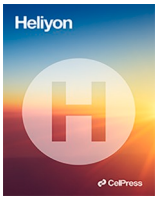

Research article

Improving the behavior of thermoplastic starch with the addition of gum Arabic: Antibacterial, mechanical properties and biodegradability

J.L. López Terán [a], Elvia V. Cabrera [a], J. Poveda [b], Judith Araque [a], M.I. Beltrán [b,*]

[a] Universidad Central del Ecuador, Facultad de Ingeniería Química, Grupo de Investigación en Alimentos, Compuestos Orgánicos, Materiales, Microbiología Aplicada y Energía (ACMME), Ciudadela Universitaria, Quito, Ecuador
[b] Departamento de Ingeniería Química, Universidad de Alicante, Apdo. 99, 03080, Alicante, Spain

ARTICLE INFO

Keywords:
Biodegradable polymers
Thermoplastic starch
Gum Arabic
Antimicrobial properties
Mechanical properties

ABSTRACT

The incorporation of different amounts of Gum Arabic (GA) in thermoplastic starch (TPS) obtained by extrusion and subsequent thermocompression has been studied. The sheets have been characterized by means of XRD, FTIR, TGA, moisture content, SEM, mechanical properties, antimicrobial activity and biodegradability via composting. The FTIR analysis of the sheets shows the presence of ester groups, while the TGA shows the presence of new processes and a residue much higher than expected is obtained. No changes in crystallinity are observed by XRD. The inclusion of GA confers antimicrobial properties to thermoplastic starch against the Gram + and Gram – bacteria studied even at the smaller concentrations. For a low GA content (0.5 and 1 g GA/100 g TPS) a homogeneous material is observed by SEM, as well as an important increase in tensile strength, modulus and deformation at break, which are very interesting properties facing the applicability of this material in single use plastics which are in contact with food or other consumable goods. At higher contents of GA, hollows and cracks appear in the material, compromising the mechanical properties. In all cases, the inclusion of GA delays the biodegradation process in soil, which can be related to its antibacterial capacity and especially in case of GA concentrations of 2 and 5 g/100 g of TPS with lower humidity of these TPS sheets.

1. Introduction

The accumulation of synthetic plastics in landfills due to their massive use and non-biodegradability, and together with the fact that they come from non-renewable resources faces our society to the challenge of finding their replacement [1]. Plastics from natural sources or biomass which are biodegradable and sustainable have been found to be a good alternative to the use of synthetic plastics [2]. In fact, in the last years some of them have been used for some interesting industrial applications, but their use is still marginal due to various technical problems that still need to be solved [3].

Starch is the second most abundant natural polymer in the world, after cellulose. Considering its biodegradability and non-toxicity to the environment, it becomes a very attractive raw material for the plastics processing industry [4]. Starch is composed of two polysaccharides based on glucose monomers; amylose, which is a linear molecule where glucose rings are associated with α-D

* Corresponding author.
E-mail address: maribel.beltran@ua.es (M.I. Beltrán).

https://doi.org/10.1016/j.heliyon.2024.e31856
Received 1 November 2023; Received in revised form 19 May 2024; Accepted 22 May 2024
Available online 27 May 2024

(1–4)-glucosan bonds, and amylopectin with a skeleton similar to amylose but containing numerous short branches with α-D (1–6)-glucose bond. The weight percentage of amylose and amylopectin varies depending on the source of starch, typically ranging from 20 to 25 % and 75–80 %, respectively. The branched chains within the amylopectin molecules contribute to the crystalline region of starch, resulting in starch granules exhibiting a degree of crystallinity ranging from 15 to 45 %. Moreover, amylose molecules are predominantly found in the amorphous regions of starch granules but are also dispersed within the crystalline phase of amylopectin clusters [5].

The technique of starch films formation by casting has been extensively used in research to obtain coatings for the food industry and for biomedical applications where different compounds are incorporated into the films to improve their barrier, mechanical, optical or antibacterial properties [6–8]. However, the preparation of starch films by casting is not viable from the industrial point of view due to the high amount of solvent to be evaporated and the impossibility of obtaining thicken films or complex shapes.

Conventional techniques utilized in the processing of synthetic plastics, such as extrusion, injection molding, and blow molding, have been effectively employed for the processing of starch-based materials and other biopolymers [9–12]. Through the application of heat, shear, and the presence of a plasticizer, the rigid original structure of starch disrupts, resulting in the formation of an uniform and homogeneous material known as thermoplastic starch (TPS). Commonly used plasticizers in starch formulations, alongside water, include glycerol, ethylene glycol, urea, and sorbitol. However, due to the significantly higher molecular weight of starch compared to synthetic polymers, the processing of starch presents greater complexity. The processing conditions and final properties of the polymer are strongly influenced by various factors such as water diffusion, granular expansion, gelatinization, melting, phase transitions, depolymerization, and retrogradation [9]. Moreover, starch is hydrophilic and the properties of the plastics obtained are quite dependent on environmental conditions, and compared to conventional plastics, lack of mechanical properties, limiting their applicability. Many of these problems can be addressed with the development of an appropriate formulation and suitable operating conditions. Some studies have been found reporting the introduction of essential oils, fibers, nanoclays or other biopolymers into TPS formulations to improve their processability, mechanical properties, barrier properties, reduce their high affinity for water, or to provide them with antioxidant or antimicrobial properties [11–16].

Gum Arabic (GA) is a natural exudate derived from Acacia trees. It is composed of a complex and branched acidic heteropolysaccharide. The main chain of GA is comprised of (1–3)-β-D-galactopyranosyl units, while its side chains consist of L-arabinofuranosyl, L-rhamnopyranosyl, D-galactopyranosyl, and D-glucopyranosyluronic acid units. In its natural form, GA exists as a mixture of calcium, magnesium, and potassium salts of the polysaccharides. Additionally, GA contains a small proportion of proteins integrated into its structure. Despite its use as an emulsifier in food, GA has large applications in the pharmaceutical industry since the broad range of health benefits reported [17,18], mainly related to its antioxidant and antimicrobial properties. Some authors have studied the antibacterial activity of GA against some bacteria species such as *Enterobacter* spp*, Enterococcus* spp*, Escherichia coli, Pseudomonas* spp*, Prevotella intermedia, Prophyromonas gingivalis, Pseudomonas aeruginosa,* and *Staphylococcus aureus*, the last two employed in this work. These authors attributed this activity to enzymes as oxidase, peroxidase and pectinase, which are present in the protein fraction of the GA [17,19]. The successful application of GA as a food coating has been demonstrated in various studies. It has proven effective in protecting against oxidation, preserving the quality, and extending the shelf life of several food items, such as bananas, papayas, mushrooms, tomatoes, Anna apples, and Indian mackerel [20–22].

Several studies have explored the preparation and characterization of gum-based starch casting films. For instance, in their work published in 2019, Cao and Song [23] utilized Karaya gum as an emulsifying and stabilizing agent in starch films. Similarly, Nandi and Guha [24], in 2018, focused on optimizing the composition of edible starch films containing guar gum to enhance properties such as tensile strength and elongation at break. Furthermore, Sapper, Talens, and Chiralt [25] conducted an analysis of the physical and barrier properties, as well as the optical properties, of edible starch films incorporating xanthan, gellan, and pullulan gums. Nevertheless, we have found only two recent works in literature where gums have been included in TPS formulations. Juan-Polo et al., 2023 [26] included peach gum in TPS, experimenting no change in mechanical properties and an improved water affinity and retarded biodegradation in soil, while Fekete and col. 2019 [27] employed agar to delay the retrogradation process of TPS. To our knowledge GA has never been employed as TPS additive.

The aim of this study was to assess the impact of incorporating varying amounts of GA on the physicochemical, mechanical, and antimicrobial properties, as well as on the biodegradability of biopolymer sheets made from potato (*Solanum tuberosum* L.) starch to obtain fully biodegradable polymers from natural sources. The sheets were manufactured using conventional techniques commonly employed for processing thermoplastic synthetic polymers, such as extrusion and thermocompression.

2. Materials and methods

2.1. Materials

Potato starch (comprising 20.5 % amylose and 79.5 % amylopectin) was procured from Finnamyl Ltd (Kokemäki, Finland). Glycerol was obtained from Labbox Labware S.L. (Vilassar de Dalt, Spain). Gum Arabic (G9752), a branched polysaccharide extracted from the acacia tree with an approximate molecular weight of 250,000, was purchased from Sigma-Aldrich. Zinc stearate was acquired from Acros Organics (Geel, Belgium).

2.2. Sheets preparation by extrusion and compression molding

To produce the TPS, potato starch was initially combined with glycerol and thoroughly stirred for 10 min at 20 °C. Subsequently,

distilled water was added and mixed again until a uniform paste was obtained. The weight ratio of each component in all the mixtures was 60/24/16 for starch/glycerol/water. As a thermal stabilizer, 1 g of zinc stearate (ZnSt) per 100 g of the aforementioned paste was incorporated. This sample was nominated as 60TPS. The required amount of Gum Arabic (GA) was added to this paste to obtain mixtures with 0.5, 1, 2 and 5 g of GA/100 g of TPS (named as 60TPS-0.5 GA; 60TPS-1GA; 60TPS-2GA and 60 TPS-5GA, respectively).

The mixtures were processed using according to the method described previously by López Terán et al. [28]. A screw extruder (Brabender Plasticorder with a PL2000 data processing unit) equipped with a 25 mm diameter screw and an L/D ratio of 2. A cylindrical die with a diameter of 2 mm was utilized. The processing conditions involved a screw speed of 80 rpm and a temperature profile ranging from 110 °C at the feeder to the die, ensuring complete gelatinization of the material. Following extrusion, the thermoplastic threads were employed in the preparation of sheets through thermo-compression using a thermos-stated hydraulic press. Approximately 40 g of the thread was placed between Kevlar sheets on a stainless-steel cylindrical mold to obtain sheets with a diameter of 16 cm and a thickness of 1 mm. The plates were set at a temperature of 152 °C for 18 min. During the initial 4 min, the press was gradually closed and opened twice to remove water vapor and prevent the formation of bubbles in the sheets. Subsequently, the pressure was increased to 8 MPa and maintained for 14 min. Finally, the sheets were cooled using a cold plate press set at 16 °C. Prior to testing, the sheets were stored for a minimum of one week at 23 °C and a relative humidity of 56 % [28]. Fig. 1 provides the photographs of the obtained sheets. All sheets exhibited high transparency, with a tendency to display a brownish color as the concentration of GA increased.

2.3. Sheets characterization

2.3.1. X-ray diffraction (XRD)

Analysis of both native starch and TPS crystalline structure was conducted using a Bruker D8-Advance diffractometer equipped with a Kristalloflex K760–80F X-ray generator and a copper anode X-ray tube. The equipment operated at 40 kV and 40 mA, and samples were scanned in the diffraction angle range of 2.5–50° with 0.05° steps increment.

2.3.2. Fourier transform infrared spectroscopy (FTIR)

This analysis was performed using the JASCO FTIR 4700 Spectrophotometer equipped with a germanium encapsulated KBr beam splitter. The spectra were recorded in the range of 4000 to 400 cm^{-1} at a resolution of 4 cm^{-1}.

2.3.3. Thermogravimetric analysis (TGA)

TGA was carried out using a PerkinElmer Pyris TGA 7 instrument equipped with Pyris software. Approximately 5 mg of the sample was placed in the sample holder and allowed to purge the ambient environment for 5 min. The temperature was then ramped from 30 to 600 °C at a rate of 10 °C/min under a nitrogen flow rate of 60 mL/min.

2.3.4. Moisture content

To determine the moisture content (MC) of the TPS samples, square pieces measuring 10 mm × 10 mm (approximately 0.6 g each) were dried in an oven at 100 °C for 24 h. The MC was calculated as the percentage difference between the initial weight and the dried weight, relative to the initial weight. Three measurements were performed for each formulation, and the mean and statistical errors were reported.

2.3.5. Scanning electron microsopy (SEM)

SEM was employed for microstructural analysis of the sheets. The analysis was conducted using a JEOL JSM-840 electron microscope with an acceleration voltage of 10 kV. Prior to imaging, the sheets were cryo-fractured by immersion in liquid nitrogen to achieve a brittle fracture surface.

2.3.6. Mechanical properties

The durometer used to measure the Shore hardness (scale A) of the TPS sheets was the Baxlo Shore A durometer. The durometer has a capacity of 0–100 Shore units and a sensitivity of 1 unit. Measurements were taken at different points on the sheets, five times in a random manner, and the average value was calculated.

A dynamometer, specifically an INSTRON 4411, was utilized to measure the maximum tensile strength, elongation at break, and Young's modulus. The tests were conducted on Halterio type sheets obtained from the original sheets. For the tensile tests, 5 samples were punched out from each sheet. The mechanical testing of the samples followed the ASTM D882-12 standard, with a jaw separation speed of 50 mm/min.

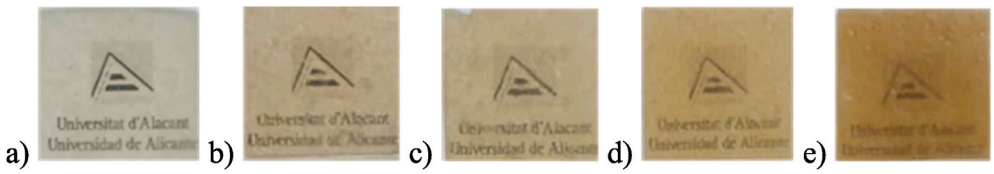

Fig. 1. Aspect of the sheets obtained; a) 60TPS, b) 60TPS-0.5 GA, c) 60TPS-1GA, d) 60TPS-2GA and e) 60TPS-5GA.

2.3.7. Antimicrobial activity using disk diffusion method

To evaluate the antimicrobial activity, the following bacterial strains were used: (a) *Staphylococcus aureus* ATCC 25923 (Gram-positive bacteria) and (b) *Pseudomonas aeruginosa* ATCC 27853 (Gram-negative bacteria). These strains were obtained from the American Type Culture Collection. Ceftazidime 30 μg Oxoid®, Erythromycin 15 μg Oxoid®, and Oxacillin 5 μg Oxoid® (Sigma-Aldrich) were used as positive controls, while water served as the negative control. Agar Mueller-Hinton from Himedia® was used in the experiments.

The agar disc method was employed to test the antibacterial activity of the sheets. All tests were performed in triplicate. The method followed is thoroughly described in a previous paper [28]. The inoculum of the bacteria was spread on Petri dishes containing agar and the discs cut from the samples where placed on them and incubated at 37 °C for 48 h. The inhibition halos formed as a consequence of the antimicrobial activity of the samples were measured and photos of the samples were taken.

2.3.8. Biodegradability in vegetable compost

The degree of disintegration was determined using an adapted version of the ISO 20200:2004 standard. The compost mixtures preparation and the details of the reactor design, sample preparations and the method for the incubation period is described in a previous paper [28]. The degree of disintegration was determined by normalizing the weight of the samples after 40 days of incubation at 40 °C with respect to their initial weight.

3. Results and discussion

3.1. X-ray diffraction

XRD patterns of potato starch and the TPS including GA are shown in Fig. 2. Potato starch presents an important diffraction peak at 2Θ angles of 17.1°, an unresolved doublet between 14.4°-15.2° and five smoother peaks at 5.7°, 11.4°, 19.8°, 22.5° and 24.1°, corresponding to a B-type crystallinity typically found in starches obtained from tubers, as has been described by other authors [29,30]. In 60TPS most of the characteristic peaks of the native potato starch disappear, remaining with a lower intensity those at 17.1 and 22.5°, indicating that, as a consequence of shear and heat applied during processing, the original B-type structure is nearly destroyed. Instead, the emergence of two new peaks at 12.9 and 19.8° suggests the formation of V_H-type crystals, as observed in the study by Altayan et al., in 2021 [31]. These researchers also indicated that the processing of TPS resulted in incomplete deconstruction of the starch granules, leading to the presence of a significant fraction of ordered recrystallized material and a smaller amorphous fraction. Other authors [26] have associated these new peaks with the interaction between the external amylopectin chains of TPS and glycerol, which is formed as a byproduct of the TPS processing. Interestingly, the inclusion of small amounts of GA does not appear to disrupt the crystallinity of the TPS.

3.2. Fourier transformed infrared spectroscopy

To investigate the binding mode between GA and TPS, the FTIR spectra of TPS components and TPS-GA were obtained. Fig. 3 shows the FTIR spectrum of the main components of TPS; starch, glycerol and GA. Due to the presence of similar functional groups, the absorption bands of the three components largely overlap, particularly in the range of 3600 to 3000 cm^{-1}, which corresponds to the wide absorption band of O–H hydroxyl stretching, 3000-2800 cm^{-1} (stretching of the CH groups of CH_3 and CH_2, respectively), 1500–1200 cm^{-1} (C–H bending) and 1200–1000 cm^{-1}(C–O stretching bands and CH_2OH related mode). The characteristic C–O–C ring vibration and C–C stretching of starch and GA lead to some absorbance bands at around 700-900 cm^{-1}. Furthermore, GA exhibited a characteristic band at 1599 cm^{-1}, which is attributed to the asymmetric stretching vibrations of the carboxyl acid salt (-COO^-, C═O, aliphatic acid) [32], while in starch the O–H bending associated with the adsorbed water in the amorphous regions causes a typical absorbance band at 1648 cm^{-1}.

In Fig. 4, the spectra of 60TPS sheets containing different amounts of GA are presented. The TPS sheets exhibit absorption bands

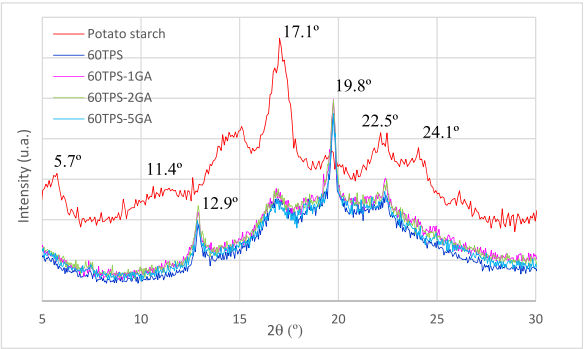

Fig. 2. XRD-patterns of starch, TPS and TPS containing different amounts of GA.

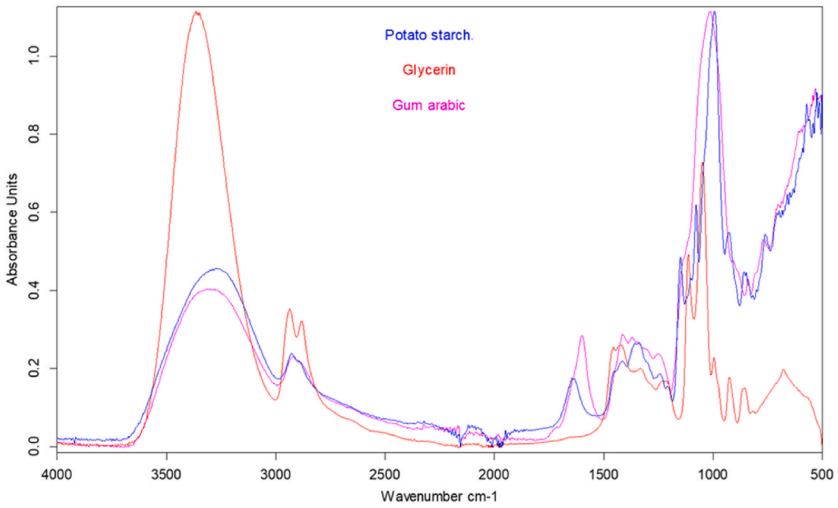

Fig. 3. FTIR spectra of potato starch, glycerin and Gum Arabic.

that correspond to the functional groups found in starch and glycerol.

All components display the absorption band of O–H stretching, which is observed at 3278 cm^{-1} in starch and 3366 cm^{-1} in glycerol. In the TPS this band is centered at 3291 cm^{-1}, between those of starch and glycerol. The analysis of the shift of this band is used to evaluate the intensity of the hydrogen bonds [31–34]. Nevertheless, due to overlapping the analysis of this band is complicated in this particular mixture; a shift to higher wavenumber with increasing GA content can be observed (from 3294 cm^{-1} in 60TPS-0.5 GA to 3299 cm^{-1} in 60TPS-5GA), which cannot be attributed exclusively to the intensity of the hydrogen bonds interaction among components since this band appears at higher wavenumbers in GA (3310 cm^{-1}).

The inclusion of GA results in notable changes in the spectra. As the GA content increases, there is a gradual intensification of the carbonyl ester band at 1717 cm^{-1}. Additionally, there is a significant increase in the intensity of the band at 1253 cm^{-1}, which is associated with C–O–C stretching in ester groups. Conversely, the intensity of the band representative of hydroxyl groups (3600-3000 cm^{-1}) decreases. These features may be due to the partial decomposition of the carbohydrates which is in accordance with the brownish aspect shown in Fig. 1. It may also indicate that crosslinking of starch and the gum may occur through esterification reactions, where glycerol could also participate. The divalent ions contained in GA may act as crosslinking agents together with the slight acidic nature of the gum and the high temperature and shear applied during TPS processing may enable the esterification reaction to occur. Some evidence about the esterification reactions between starch and gums have been described in the literature.

Cao and Song [23] noted the presence of a small band at 1722 cm^{-1} and 1246 cm^{-1} in starch films prepared by casting that incorporated karaya gum. In a separate study, Morán et al. [35] reported the appearance of bands at 1703 cm^{-1} and 1240 cm^{-1} following the modification of starch with acetic acid and maleic anhydride.

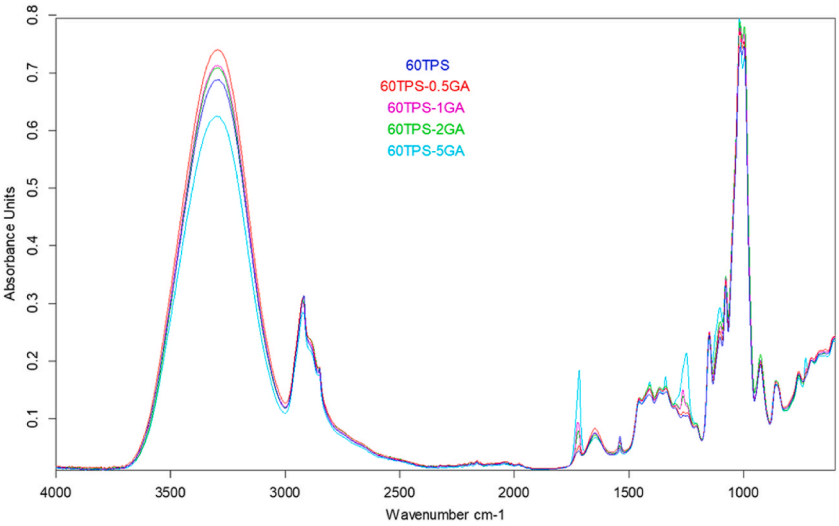

Fig. 4. FTIR spectra of 60TPS, 60TPS-0.5 GA, 60TPS-1GA, 60TPS-2GA y 60TPS-5GA sheets.

3.3. Thermogravimetric analysis

Fig. 5 illustrates the TG curves of 60TPS, GA, and 60TPS-5GA. In the TG curve of 60TPS, an initial process is observed between 100 and 240 °C, which corresponds to the partial loss of volatile compounds present in TPS, such as water and glycerin. The main decomposition peak of 60TPS occurs between 240 and 370 °C, with a maximum decomposition rate temperature (T_{max}) of 319.5 °C, also showing two distinct shoulders. The main decomposition process is associated with the depolymerization of the amylose and amylopectin chains that constitute starch, resulting in the breakdown of glucose rings [36]. It is also related to the evaporation or decomposition of glycerin and water associated with starch as a consequence of the gelatinization process. Similarly, Liu et al. [33] described four different processes in the thermal decomposition of TPS including sisal fiber. The carbonaceous residue obtained is 9.1 % at 600 °C. On the other hand, GA presents an initial process between 40 and 140 °C in which the evaporation of moisture occurs. Then the decomposition of carbohydrates forming GA and the further decomposition of glucose formed take place [22] process occurs at lower temperatures than in TPS, with a T_{max} of 315.5 °C but in a wider range of temperatures and presents a residue of 25.9 %, much higher than that of TPS.

Fig. 5 also includes the experimental TG curve of 60TPS-5GA and the theoretical curve 60TPS-5GA (dotted line) obtained as the sum of the mass data of 60TPS and GA weighted by the composition of each of them in the 60TPS-5GA formulation. As expected this theoretical curve has a shape very similar to that of 60TPS given the greater weight of this component in the mixture (100 parts of TPS versus 5 parts of GA), presenting its T_{max} at 319.5 and a residual weight of 9.9 % at 600 °C, very close to those of TPS. Nevertheless, observing the experimental 60TPS-5GA curve it can be appreciated that incorporation of GA significantly modifies the experimental decomposition of TPS. The residue obtained is much higher than expected by the theoretical mixture of the components. For 60TPS-5GA an experimental value for the residue at 600 °C of 15.6 % is obtained compared to 9.9 % mentioned above.

Fig. 6 shows the DTG curves of the sheets containing different amounts of GA and that of 60TPS. The T_{max} are reduced well above those expected with due to addition of GA to TPS, obtaining values of 318.9, 318.4, 316.4 and 313.0 °C with an addition of GA of 0.5, 1, 2 and 5 g of GA/100 g of TPS, which are even lower than that of GA itself. It is again observed, that there are important modifications in the behavior of TPS which must be a consequence of the esterification reactions that may occur between the TPS components as observed by FTIR, leading to a slight reduction in the thermal stability of TPS.

3.4. Moisture content

Table 1 shows the equilibrium moisture values of the sheets stored at 23 °C in an environment with 56 % humidity during one week. The inclusion of GA in the TPS produces a reduction in the moisture of the sheets, which is greater than 25 % in 60TPS-2GA and 60TPS-5GA. A decrease in the values of the moisture content in equilibrium with the environmental humidity is very interesting for biodegradable materials since it allows major stability of the properties of the biomaterials and prevents premature degradation, which generates greater durability [24]. As water acts as plasticizer for starch, water content changes markedly influence the mechanical behavior of the sheets.

The reduction in equilibrium moisture content observed is consistent with the ester formation due to crosslinking between GA and starch, which has been mentioned above. Ester formation implies a reduction of free hydroxyl groups capable of forming hydrogen bonds with water and so the TPS affinity for water.

The value of moisture content found in literature when gums are employed to prepare films of starch obtained by casting are quite scattered. Cao and Song [23] also found a reduction in films moisture with the inclusion of guar gum whilst Sapper et al. [25], described a reduction of equilibrium moisture content for films which included gellan gum, and no effect for xanthan gum. In a similar manner, Martins et al. [37] investigated the incorporation of k-carrageenan and locust bean gum into edible starch films. They

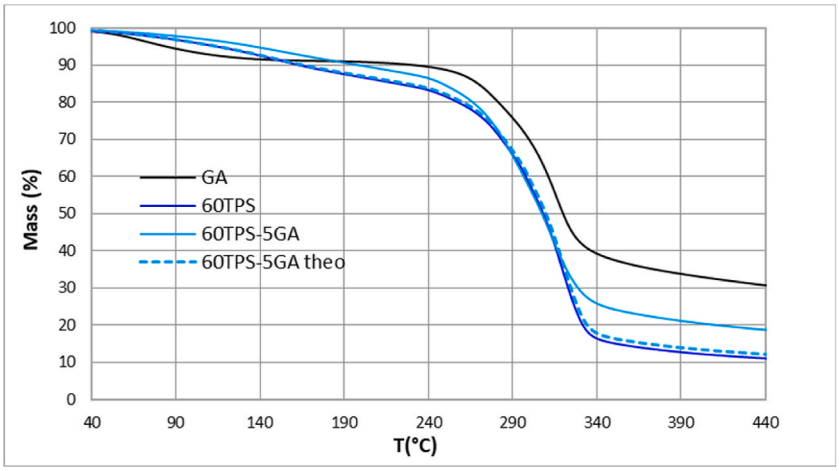

Fig. 5. TG curves of the sheets containing GA, 60TPS, 60TPS-5GA and 60TPS-5GA theoretical.

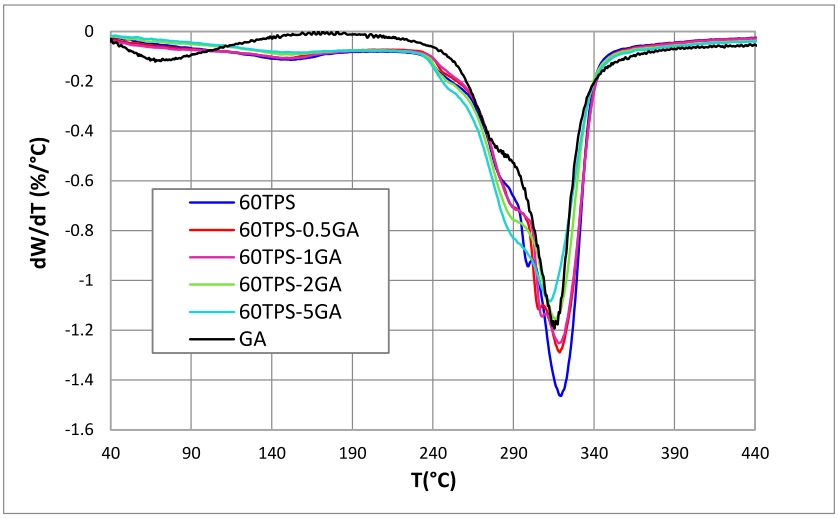

Fig. 6. DTG curves of the sheets containing different amounts of GA along with that of 60TPS.

Table 1
Physical and mechanical properties of the TPS sheets containing GA.

Sample	Moisture content (%)	Hardness (Shore A)	Tensile Strenght (MPa)	Young's Modulus (MPa)	Elongation at break (%)
60TPS	15.4 ± 0.3	86.7 ± 0.7	2.5 ± 0.5	11.3 ± 0.8	53.5 ± 7.0
60TPS-0.5 GA	14.4 ± 0.3	87.3 ± 0.5	4.1 ± 0.3	13.3 ± 1.1	72.7 ± 8.9
60TPS-1GA	14.3 ± 0.5	88.3 ± 0.7	4.5 ± 0.1	13.2 ± 1.7	82.3 ± 3.4
60TPS-2GA	11.4 ± 0.1	89.3 ± 0.7	2.7 ± 0.3	5.2 ± 0.3	137.0 ± 7.9
60TPS-5GA	11.4 ± 0.3	89.3 ± 0.7	2.1 ± 0.2	4.3 ± 0.9	212.7 ± 24.3

observed a decrease in moisture content, which was attributed to the reduced availability of hydroxyl groups due to crosslinking between the gum and polymer chains. However, Nandi and Guha reported an increase in moisture content of starch films with increasing guar gum content. This was explained by the viscosity increase in the film solution, leading to higher water retention [24]. The structure of gums allows for both hydrophilic and hydrophobic interactions, and the physicochemical response of gums can be explained by the balance between these interactions within each material. The functional properties of gums are closely tied to their structure, which influences characteristics such as solubility, viscosity, interaction with water and oil in emulsions, and the ability to microencapsulate, among others [17,22].

3.5. SEM

Fig. 7 shows the SEM images of the starch (Fig. 7a) and GA (Fig. 7b) granules at 1000× magnifications and the fractured surface of 60TPS, 60TPS-0.5 GA, 60TPS-1GA, 60TPS-2GA and 60TPS-5GA sheets at 5000× magnifications. The 60TPS sheet has a homogeneous appearance, both on the fracture surfaces shown in Fig. 7c, and also on the external surface (not shown). The presence of starch granules (Fig. 7a) is not observed in the sheets, demonstrating that during the extrusion process the de-structuring of the starch grains occurred, allowing interaction with glycerin and water to obtain a continuous material. GA is a very soluble material in water that may be dissolved during processing, and no GA particles are expected to be observed in TPS sheets. The 60TPS-0.5 GA (Fig. 7d) and 60TPS-1GA (Fig. 7e) material has a similar appearance to 60TPS; a homogeneous material is seen on the fracture surface which demonstrates good incorporation of GA into the sheet. On the other hand, Fig. 7f shows that by increasing the amount of GA to 2 g/100 g of TPS an irregular surface is obtained which may be the result of GA saturation in the sheet and small voids can be visualized. As the content of GA increase to 5 g/100 g of TPS (Fig. 7g) some cracks can be observed and the voids become greater which could be related to the premature decomposition or crosslinking reactions of the polymers, as mentioned above.

3.6. Mechanical properties

Table 1 presents the mechanical properties of TPS sheets with varying contents of GA. The Shore A hardness shows that TPS is a soft material in the range of most of thermoplastic rubbers. The inclusion of the amount of the gum produces an increase in the Shore A hardness specially at low contents of GA.

The addition of GA to the 60TPS matrix results in an increase in both tensile strength and Young's Modulus, which reaches a maximum at 1 g GA/100 g TPS. The good incorporation of low contents of the gum and the crosslinking between starch and gum

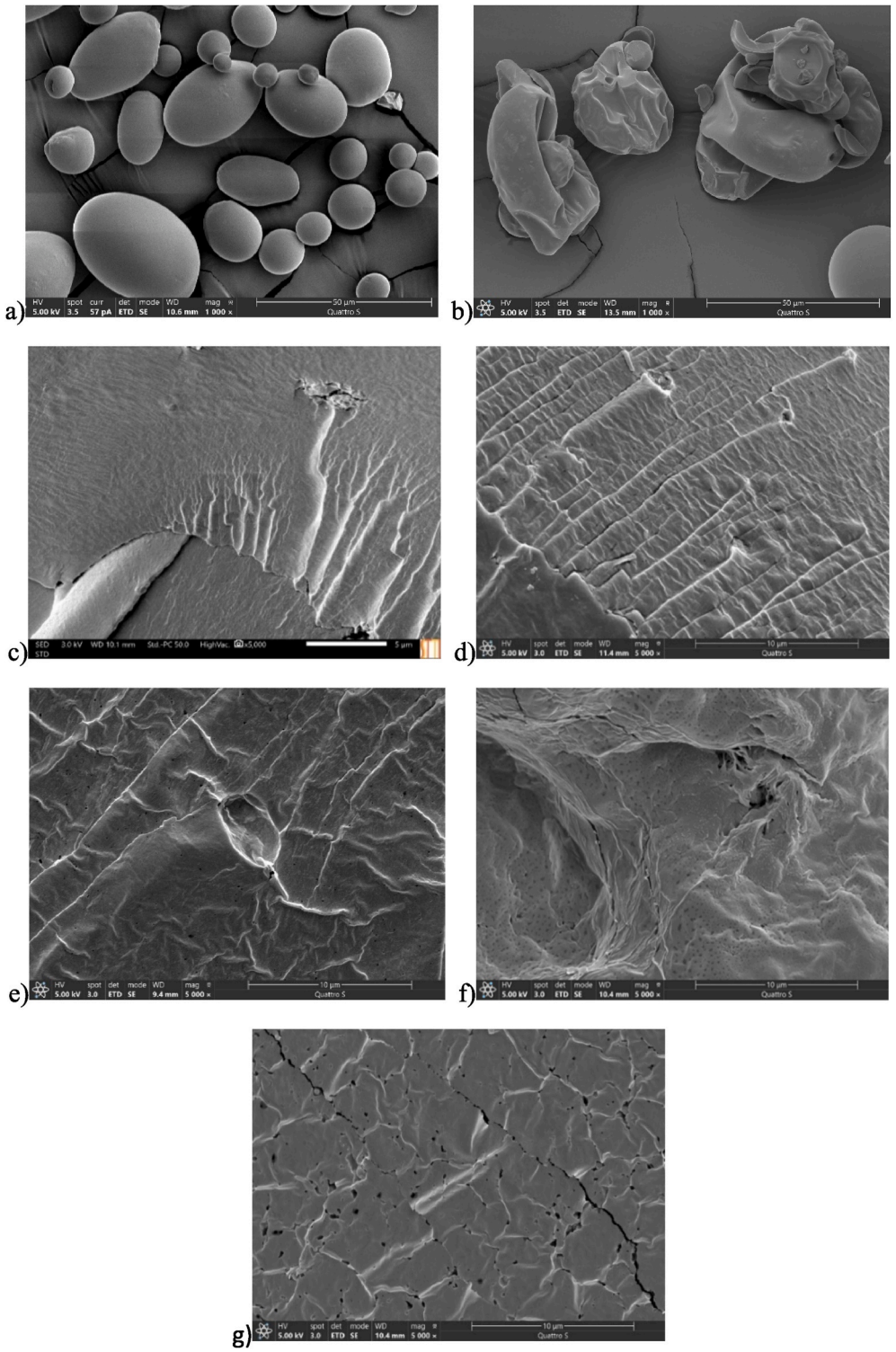

Fig. 7. SEM photographs at 1000× magnifications of (a) starch granules, (b) GA granules (c) 60TPS, (d) 60TPS-0.5 GA, (e) 60TPS-1GA, (f) 60TPS-2GA and (g) 60TPS-5GA at 5000× magnifications.

discussed above may contribute to developing a more resistant network. As the content of gum increases over 1 g of GA/100 g of TPS, tensile strength and Modulus decreases, which could be related to an excess of this component not incorporated properly, as observed in SEM photographs. In addition, the presence of voids and cracks within the sheets can have a detrimental impact on the mechanical

properties of the material. Unexpectedly, elongation at break increases significantly with GA content, with a regression coefficient of 0.98.

As commented, the literature on the preparation of films obtained by casting is quite extensive, not being the case of TPS thermoformed sheets. The findings presented in this work are in alignment with those previously reported by Mendes et al., 2016 (2.1 MPa, 69 % and 39 MPa for tensile strength, elongation and modulus, respectively) for a formulation equivalent to our 60TPS but employing corn starch instead of potato starch [11]. Juan-Polo et al., 2023 [26] included peach gum in TPS obtained by injection molding but did not observe any remarkable change in mechanical properties with the content of gum. These authors presented similar values of elongation at break and tensile strength for TPS, while Young's Modulus values were much higher than those presented in this work. In any case, the difficulty in comparing mechanical properties should be borne in mind since factors such as preparation conditions, homogeneity of the sheet, test speed, geometry of the specimen, cracks, impurities, thickness of the sheet, may have influence in the results.

3.7. Antimicrobial assay

Table 2 shows the size of the inhibition area after 48 h of incubation of bacteria *Staphylococcus aureus* and *Pseudomonas aeruginosa* in agar when discs of TPS and TPS containing GA are introduced into the media. The photos of the inhibition halos are included as supplementary material. The TPS discs show no antibacterial activity against any of the bacteria tested, but when GA is included in the TPS, all discs show inhibition halos, even at the lowest GA content.

The GA is able to maintain its antibacterial activity after mixing and processing with the other components of TPS, indicating that the protein fraction of the GA responsible for its antibacterial activity [17,19] is not altered by the processing conditions of the sheets and may not participate in crosslinking between GA and the other components of TPS. A particular behavior was observed since the antimicrobial activity increased with increased the concentration of GA up to 2 g of GA/100 g of TPS and then the halo decreased when increasing the concentration to 5 g of GA/100 g TPS. Martinez- Bustos (2014) [39], described a saturating effect of the substrate when some organic compounds are employed as antimicrobial agents. This behavior can be attributed to the kinetics of saturation by the substrate, which is typical of the enzymatic activity responsible for the antimicrobial behavior that have been proposed for the action of various organic compounds.

In general, all the samples show a higher inhibition against *Pseudomonas aeruginosa*, with is considered more resistant than the Gram positives bacteria since its external membrane avoids the diffusion of hydrophobic molecules.

Other authors have successfully included low concentrations of Essential Oils in TPS [38] and starch casting films [39,40] to confer them antibacterial properties, especially for applications where the bioplastic is in contact with food. Nevertheless, these oils are terpene or benzene derivatives and have a particular odor and change organoleptic characteristics of food which is not the case of GA [16].

3.8. Biodegradability in compost

Fig. 8 shows the residual weight of the sheets subjected to composting for 10, 20, 30 and 40 days. During composting starch is degraded by biological processes, especially by enzymatic fermentation which leads the breakdown of long chain sugars to smaller fragments, conducting to the progressive deterioration and disintegration of the samples, and to the formation of CO_2, new biomass and water. Under the conditions of composting due to the effect of humidity and temperature in the reactor the disintegration is accelerated. The rate of degradation depends not only on the test conditions but also on the composition of the mixture.

The 60TPS decomposes fast presenting a residual weight of 38 % after 20 days of composting. The inclusion of GA in TPS significantly slows the degradation process. The higher the GA content the slower the degradation process. For example, on day 20 the residual weight is 44, 60, 63 and 70 % for GA contents of 0.5, 1, 2 and 5 g/100 g TPS, respectively. After 40 days of testing, the 60TPS-5GA sample maintains a residual weight of 4 % while the rest of the samples have been completely disintegrated with 60TPS and 60TPS-0.5 GA having disintegrated probably days before. The antimicrobial effect conferred by GA together with the lower affinity by water, especially for 60TPS-2GA and 60 TPS-5GA may be responsible for delaying microbial attack during composting of samples.

Table 2
Antimicrobial activity of the TPS sheets containing GA against Gram-positive *Staphylococcus aureus* and Gram-negative *Pseudomonas aeruginosa*.

TPS Sheets	Inhibition zone *S. aureus* (mm)	Inhibition zone *P. aeruginosa* (mm)
60TPS	–	–
60TPS-0.5 GA	8.3 ± 3.3	13.0 ± 3.1
60TPS-1GA	13.3 ± 1.3	11.5 ± 1.2
60TPS-2GA	17.0 ± 0.5	17.8 ± 0.6
60TPS-5GA	12.0 ± 0.2	12.3 ± 0.2
Positive control Eritromicin (15 μg)	22.0 ± 7.0	–
Oxacilin (5 μg)	33.0 ± 7.0	–
Ceftazidime (30 μg)	–	35.0 ± 7.00

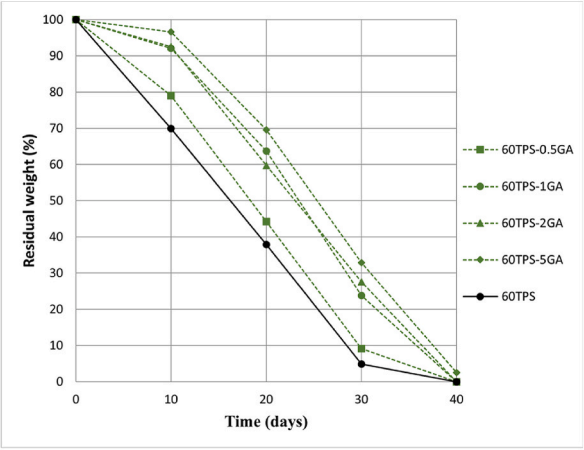

Fig. 8. Residual weight curves of the 60TPS sheets containing different amounts of GA.

There are few results in the literature studying the biodegradation of TPS in soils. For example, Sessini et al., 2019 [41] found in a TPS with 68 % pea starch that after 20 days 40 % of the weight of the sample had been lost, achieving a total degradation after 60 days, while Zain et al., 2018 [42] found that the weight loss was greater than 50 % after 20 days of trial in a TPS containing 65 % cassava starch. The results shown for our TPS with 60 % potato starch are between those reported. As mentioned, Juan-Polo et al. (2023) [26] included peach gum in TPS; these authors found a faster disintegration with the inclusion of the gum. Contrarily to the effect observed for GA, the peach gum increased the water affinity of their TPS, justifying the differences in biodegradation in soil found.

4. Conclusions

The incorporation of GA to TPS leads to important modifications in the physical and mechanical properties of the sheets. The FTIR spectra indicate the formation of ester groups from the hydroxyl groups of starch and carboxylic acids of GA, which may be related to the partial decomposition or crosslinking between both biopolymers after processing by extrusion and thermocompression. These esterification reactions result in a reduction of the free hydroxyl groups, leading to a lower affinity for water. As a result, the equilibrium humidity of these materials with the environment is reduced with the incorporation of GA, which is very interesting from the point of view of the stability with the environmental conditions of this biomaterial. With the incorporation of the gum, the TG curves of the sheets containing GA present important modifications in comparison to the components alone (TPS and gum), which is consistent with the changes observed by FTIR which involves a small reduction in their thermal stability. By means of SEM a homogeneous fracture surface has been observed for the sheets containing up to 1 g GA per 100 g of TPS, while at higher concentrations there are holes and cracks. Especially the resistance strength and also the elongation at break increase up to this gum content. All sheets containing GA have antimicrobial activity against Gram positive bacteria *Staphylococcus aureus* ATCC 25923 and Gram negative *Pseudomonas aeruginosa* ATCC 27853. The biodegradation rate in soil is observed to be slower with higher GA content, likely due to the lower equilibrium moisture of the samples and the antimicrobial properties of GA on this biomaterial. The incorporation of GA into TPS results in a biopolymer that could serve as a viable alternative for designing new biodegradable products. This biopolymer is useful for manufacturing single-use products that require antimicrobial properties.

Data availability statement

The data generated in this research may be sent to the requesting party with substantiated justification.

CRediT authorship contribution statement

J.L. López Terán: Writing – original draft, Visualization, Methodology, Investigation, Data curation. **Elvia V. Cabrera:** Writing – original draft, Visualization, Supervision. **J. Poveda:** Writing – original draft, Investigation. **Judith Araque:** Validation, Investigation. **M.I. Beltrán:** Writing – review & editing, Supervision, Resources, Methodology, Conceptualization.

Declaration of competing interest

The authors declare the following financial interests/personal relationships which may be considered as potential competing interests: Jorge L. Lopez reports financial support was provided by Central University of Ecuador. If there are other authors, they declare that they have no known competing financial interests or personal relationships that could have appeared to influence the work reported in this paper.

Acknowledgements

The authors would like to express their gratitude to the "Convenio-Programa de Doctorado en Ingeniería Química de la Universidad Central del Ecuador (Quito-Ecuador)" and the University of Alicante (Alicante-Spain) for their support.

References

[1] D. Patel, D. Mamtora, A. Kamath, A. Shukla, Rogue one: a plastic story, Mar. Pollut. Bull. 177 (2022) 113509.
[2] J.R. Westlake, M.W. Tran, Y. Jiang, X. Zhang, A.D. Burrows, M. Xie, Biodegradable biopolymers for active packaging: demand, development and directions, Sustainable Food Technol 1 (2023) 50–72.
[3] E. Lizundia, F. Luzi, D. Puglia, Organic waste valorization towards circular and sustainable biocomposites, Green Chem. 24 (2022) 5429–5459.
[4] S.M. Emadian, T.T. Onay, B. Demirel, Biodegradation of bioplastics in natural environments, Waste Manag. 59 (2017) 526–536.
[5] A. Surendren, A.K. Mohanty, Q. Liu, M.A. Misra, A review of biodegradable thermoplastic starches, their blends and composites: recent developments and opportunities for single-use plastic packaging alternatives, Green Chem. 24 (2022) 8606–8636.
[6] M.C. Gutiérrez, M.C. Nuñez-Santiago, M. Romero-Bastida, C.A. Martinez-Bustos, Effects of coconut oil concentration as a plasticizer and *Yucca schidigera* extract as a surfactant in the preparation of extruded corn starch films, Starch – Stärke 66 (2014) 1079–1088.
[7] J.A. Do Evangelho, G. da Silva Dannenberg, B. Biduski, S.L.M. El Halal, D.H. Kringel, M.A. Gularte, A.M. Fiorentini, E. Da Rosa Zavareze, Antibacterial activity, optical, mechanical, and barrier properties of corn starch films containing orange essential oil, Carbohydr. Polym. 222 (2019) 114981.
[8] C. Medina-Jaramillo, O. Ochoa-Yepes, C. Bernal, L. Famá, Active and smart biodegradable packaging based on starch and natural extracts, Carbohydr. Polym. 176 (2017) 187–194.
[9] H. Liu, F. Xie, L. Yu, L. Chen, Thermal processing of starch-based polymers, Prog. Polym. Sci. 31 (2009) 1348–1368.
[10] A.M. Salaberria, J. Labidi, S.C. Fernandes, Chitin nanocrystals and nanofibers as nano-sized fillers into thermoplastic starch-based biocomposites processed by melt-mixing, Chem. Eng. J. 256 (2014) 356–364.
[11] J.F. Mendes, R.T. Paschoalin, V.B. Carmona, A.R. Sena-Neto, A.C.P. Marques, J.M. Marconcini, L.H.C. Mattoso, E.S. Medeiros, J.E. Oliveira, Biodegradable polymer blends based on corn starch and thermoplastic chitosan processed by extrusion, Carbohydr. Polym. 137 (2016) 452–458.
[12] Y. Kong, S. Qian, Z. Zhang, J. Tian, The impact of esterified nanofibrillated cellulose content on the properties of thermoplastic starch/PBAT biocomposite films through ball-milling, Int. J. Biolog. Molec. 253 (2023) 127462.
[13] V.M. Azevedo, R.A. Carvalho, S.V. Borges, P.I.C. Claro, F.K. Hasegawa, M.I. Yoshida, J.M. Marconcini, Thermoplastic starch/whey protein isolate/rosemary essential oil nanocomposites obtained by extrusion process: antioxidant polymers, J. Appl. Polym. Sci. 136 (23) (2019) 47619.
[14] L.A. Castillo, O.V. López, J. Ghilardi, M.A. Villar, S.E. Barbosa, M.A. García, Thermoplastic starch/talc bionanocomposites. Influence of particle morphology on final properties, Food Hydrocolloids 51 (2015) 432–440.
[15] I. Derungs, M. Rico, J. López, Barral, L. Montero, B. Bouza, Influence of the hydrophilicity of montmorillonite on structure and properties of thermoplastic wheat starch/montmorillonite bionanocomposites, Polym. Adv. Technol. 32 (11) (2021) 4479–4489.
[16] S.P. Bangar, W.S. Whiteside, A.O. Ashogbon, Recent advances in thermoplastic starches for food packaging: a review. Food Pakag, Shelf Life. 30 (2021) 100743.
[17] A.A. Aloqbi, Gum Arabic as a natural product with antimicrobial and anticancer activities, Arch. Pharm. Pract. 11 (2) (2020) 107–112.
[18] T.H. Musa, I.H. Musa, W. Osman, M.C. Campbell, H.H. Musa, A bibliometric analysis of global scientific research output on Gum Arabic, Bioact. Carbohydr. Diet. Fibre. 25 (2021) 100254.
[19] S.H. Baien, J. Seele, T. Henneck, C. Freibrodt, G. Szura, H. Moubasher, R. Nau, G. Brogden, M. Mörgelin, M. Singh, M. Kietzmann, M. von Köckritz-Blickwede, N. de Buhr, Antimicrobial and immunomodulatory effect of gum Arabic on human and bovine granulocytes against *Staphylococcus aureus* and *Escherichia coli*, Front. Immunol. 10 (2020) 1–18.
[20] A. Ali, M. Maqbool, S. Ramachandran, P.G. Alderson, Gum Aabic as a novel edible coating for enhancing shelf-life and improving postharvest quality of tomato (*Solanum lycopersicum L.*) fruit, Postharvest Biol. Technol. 58 (1) (2010) 42–47.
[21] M. Maqbool, A. Ali, P.G. Alderson, M.T. Muda-Mohamed, Y. Siddiqui, N. Zahid, Postharvest application of gum Arabic and essential oils for controlling anthracnose and quality of banana and papaya during cold storage, Postharvest Biol. Technol. 62 (1) (2011) 71–76.
[22] N. Prasad, N. Thombare, S.C. Sharma, S. Kumar, Gum Arabic – a versatile natural gum: a review on production, processing, properties and applications, Ind. Crop. Prod. 187 (Part A) (2022) 115304.
[23] T.L. Cao, K.B. Song, Effects of gum karaya addition on the characteristics of loquat seed starch films containing oregano essential oil, Food Hydrocolloids 97 (2019) 105198.
[24] S. Nandi, P. Guha, Modelling the effect of guar gum on physical, optical, barrier and mechanical properties of potato starch based composite films, Carbohydr. Polym. 200 (2018) 498–507.
[25] M. Sapper, P. Talens, A. Chiralt, Improving functional properties of cassava starch-based films by incorporating xanthan, gellan, or pullulan gums, Int. J. Polym. Sci. (2019) 5367164.
[26] A. Juan-Polo, C. Pavón, H. Rosa-Ramírez, J. López-Martínez, Use of raw peach gum as a sustainable additive for the development of water-sensitive and biodegradable thermoplastic starch films, Polymers 15 (2023) 3359.
[27] E. Fekete, E. Bella, E. Csiszár, J. Móczó, Improving physical properties and retrogradation of thermoplastic starch, Int. J. Biolog. Molec. 136 (2019) 1036, 1033.
[28] J. López, E. Cabrera, J. Araque, J. Poveda, M. Beltrán, Development of antibacterial thermoplastic starch with natural oils and extracts: structural, mechanical and thermal properties, Polymers 16 (2024) 180.
[29] V.K. Shivaraju, S. Valla yil Appukuttan, Sunny Kumar, The influence of bound water on the FTIR characteristics of starch and starch nanocrystals obtained from selected natural sources, Starch - Stärke 71 (5–6) (2019).
[30] D. Domene-López, J.C. García-Quesada, I. Martin-Gullon, M.G. Montalbán, Influence of starch composition and molecular weight on physicochemical properties of biodegradable films, Polymers 11 (2019) 1084.
[31] M. Mhd Altayan, T. Al Darouich, F. Karabet, Thermoplastic starch from corn and wheat: a comparative study based on amylose content, Polym. Bull. 78 (6) (2021) 3131–3147.
[32] H. Espinosa-Andrews, O. Sandoval-Castilla, H. Vázquez-Torres, E.J. Vernon-Carter, C. Lobato-Calleros, Determination of the gum Arabic–chitosan interactions by Fourier Transform Infrared Spectroscopy and characterization of the microstructure and rheological features of their coacervates, Carbohydr. Polym. 79 (3) (2010) 541–546.
[33] Y. Liu, L. Liao, J. Xiong, Z. Liang, Thermal degradation behavior and structures of thermoplastic cassava starch/sisal fiber composites, Polym. Compos. 43 (4) (2022) 2022–2033.
[34] K. Shivaraju, V. Appukuttan, S. Kumar, The influence of bound water on the FTIR characteristics of starch and starch nanocrystals obtained from selected natural sources, Starch - Stärke 71 (2018) 1700026.
[35] J.I. Morán, A. Vázquez, V.P. Cyras, Bio-nanocomposites based on derivatized potato starch and cellulose, preparation and characterization, J. Mater. Sci. 48 (20) (2013) 7196–7203.
[36] M. Piglowska, B. Kurc, L. Rymaniak, P. Lijewski, P. Fuć, Kinetics and thermodynamics of thermal degradation of different starches and estimation the OH group and H_2O content on the surface by TG/DTG-DTA, Polymers 12 (2) (2020) 357.
[37] J.T. Martins, M.A. Cerqueira, A.I. Bourbon, A.C. Pinheiro, B.W.S. Souza, A.A. Vicente, Synergistic effects between k-carrageenan and locust bean gum on physicochemical properties of edible films made thereof, Food Hydrocolloids 29 (2012) 280–289.

[38] X. Zhang, H. Ma, W. Qin, B. Guo, P. Li, Antimicrobial and improved performance of biodegradable thermoplastic starch by using natural rosin to replace part of glycerol, Ind. Crop. Prod. 178 (2022) 114613.
[39] F. Martinez-Bustos, Effects of coconut oil concentration as a plasticizer and Yucca schidigera extract as a surfactant in the preparation of extruded corn starch films, Starch - Stärke 66 (11–12) (2014) 1079–1088.
[40] Y. Shen, J. Zhou, C. Yang, Y. Chen, Y. Yang, C. Zhou, L. Wang, G. Xia, X. Yu, H. Yang, Preparation and characterization of oregano essential oil-loaded *Dioscorea zingiberensis* starch film with antioxidant and antibacterial activity and its application in chicken preservation, Int. J. Biol. Macromol. 212 (2022) 20–30.
[41] V. Sessini, M.P. Arrieta, J.M. Raquez, P. Dubois, J.M. Kenny, L. Peponi, Thermal and composting degradation of EVA/Thermoplastic starch blends and their nanocomposites, Polym. Degrad. Stabil. 159 (2019) 184–198.
[42] A.H.M. Zain, M.K. Ab Wahab, H. Ismail, Biodegradation behaviour of thermoplastic starch: the roles of carboxylic acids on cassava starch, J. Polym. Environ. 26 (2) (2018) 691–700.